

This is the **accepted version** of the article:

Arias-Martorell, Julia; Zeininger, Angel; Kivell, Tracy L. «Trabecular structure of the elbow reveals divergence in knuckle-walking biomechanical strategies of African apes». *Evolution*, (September 2021). DOI 10.1111/evo.14354

This version is available at <https://ddd.uab.cat/record/249696>

under the terms of the  **CC BY** COPYRIGHT license

1 **Trabecular structure of the elbow reveals divergence in knuckle-walking biomechanical**
2 **strategies of African apes**

3 Julia Arias-Martorell^{1,2*}, Angel Zeininger³, Tracy L. Kivell^{2,4}

4 1. Institut Català de Paleontologia Miquel Crusafont, Edifici ICTA-ICP, Carrer Columnes
5 s/n, Campus de la UAB, Universitat Autònoma de Barcelona, 08193 Cerdanyola del Vallès,
6 Barcelona, Spain.

7 2. Animal Postcranial Evolution (APE) Lab, School of Anthropology and Conservation,
8 Marlowe Building, University of Kent, Canterbury, CT2 7NR, UK

9 3. Department of Evolutionary Anthropology, Duke University, Durham, North Carolina,
10 27708, USA.

11 4. Department of Human Evolution, Max Planck Institute for Evolutionary Anthropology,
12 Deutscher Platz 6, Leipzig, Germany 01403, Germany

13

14 *Corresponding author: Dr Julia Arias-Martorell

15 Correspondence to: julia.arias@icp.cat

16

17 **Running Head:** Trabecular structure of the African ape elbow

18

19 **Abstract**

20 African apes engage in a distinct form of locomotion called knuckle-walking, but
21 there is much ambiguity as to when and how this locomotor behaviour evolved. This study
22 aims to elucidate potential differences in knuckle-walking elbow posture and loading in
23 African apes through the study of trabecular bone. Using a whole-epiphysis approach, we
24 quantified variation in trabecular structure of the distal humerus of chimpanzees, western
25 lowland gorillas, and mountain gorillas in comparison to orang-utans, siamangs and a sample

26 of Old and New World monkeys. Results demonstrate differences in the distribution of
27 trabecular bone within the distal humerus that are consistent across taxa that habitually use a
28 flexed-elbow posture in comparison to those that use an extended-elbow during locomotion.
29 Western lowland gorillas show an extended-elbow pattern consistent with the straight
30 forelimb position during knuckle-walking, whereas chimpanzees show a flexed-elbow
31 pattern. Unexpectedly, mountain gorillas show an intermediate pattern between their western
32 counterparts and chimpanzees. The differences found in elbow joint posture between
33 chimpanzees and gorillas, and between gorilla species, point to diversification in the knuckle-
34 walking biomechanical strategies among African apes, which has implications in the debate
35 regarding the locomotor behaviour from which human bipedalism arose.

36

37 **Keywords:** bone functional adaptation; joint posture; hominoid; locomotion; chimpanzee;

38 gorilla

39

40 **Introduction**

41 Knuckle-walking is the most frequent form of locomotion used by African apes
42 (Hunt, 1991; Doran, 1996; Doran, 1997; Remis, 1995). In this quadrupedal locomotion, the
43 hand is in a vertical posture with the digits flexed such that weight is born on the dorsal side
44 of the intermediate phalanges of the second to fifth rays. Although there is variation across
45 genera and species in how often knuckle-walking is used, all African apes knuckle-walk both
46 on the ground and in trees at least 85% of their locomotor time (Hunt, 1991; Doran, 1997;
47 Crompton et al., 2010). As such, there has been much discussion about the potential adaptive
48 and evolutionary significance associated with this distinct form of locomotion (reviewed in
49 Richmond et al., 2001). The presence or absence of potential knuckle-walking adaptations,
50 particularly of the wrist and hand, is a dominant feature in debates about the locomotor
51 behaviour of the last common ancestor of *Pan* (i.e., chimpanzees and bonobos) and hominins
52 and whether knuckle-walking might have independently evolved in gorillas and chimpanzees
53 (Begun, 1992; Richmond and Strait, 2002; Dainton and Macho, 1999; Kivell and Schmitt,
54 2009; Lovejoy, 2009; Williams, 2010). As an alternative to external features associated with
55 the hand and wrist, this study aims to identify variation in the internal anatomy (trabecular
56 structure) at the elbow (distal humerus) in extant African apes to investigate the presence of a
57 knuckle-walking signal.

58 The external elbow morphology of primates provides stability in a wide range of
59 pronation-supination and flexion-extension movements (Rose, 1988; Drapeau, 2008). Of
60 particular importance is the distal humerus, which articulates with both forearm bones and for
61 which extant apes, including humans, share a derived morphology with a spool-shaped
62 trochlea (which articulates with the ulna) and a globular capitulum (which articulates with the
63 radius) (Supporting Information [SI] Fig. S1). Morphological variation of the distal humerus
64 across apes is traditionally thought to reflect their locomotor differences (Rose, 1988;

65 Drapeau, 2008). Relative to more suspensory Asian apes (Schmitt, 1994; Zihlman et al.,
66 2011), African apes have more distally expanded and flatter joints to sustain loading of the
67 forelimb during terrestrial locomotion with an extended forearm (Drapeau, 2008). Powerful
68 forearm flexor and extensor muscles, which are essential during below-branch locomotor
69 behaviours and which generate transverse forces that are resisted by the spool-shaped
70 trochlear morphology, insert on the medial and lateral epicondyles of the distal humerus.

71 External bone morphology, and particularly joint morphology, is potentially more
72 genetically constrained compared with internal bone architecture (Rafferty and Ruff, 1994;
73 Lieberman et al., 2001). Experimental evidence demonstrates that trabecular bone in
74 particular can respond to the magnitude, frequency and direction of mechanical load during
75 life (Biewener et al., 1996; Pontzer et al., 2006; Barak et al., 2011; reviewed in Kivell, 2016).
76 Although other non-functional factors can influence trabecular structure, such as genetics
77 (Ryan et al., 2017), age (Macho et al., 2005), hormones (Khosla et al., 2006) or systemic
78 differences (Tsegai et al., 2018), numerous comparative studies have demonstrated strong
79 correlations between variation in trabecular structure and differences in behaviour among
80 primates in many bones/joints of the postcranial skeleton (e.g., Ryan and Shaw, 2012; Tsegai
81 et al., 2013; Saers et al., 2019). The proximal humerus has been the anatomical focus of many
82 of these studies, with some showing clear functional signals within the trabecular structure
83 across primates (Rafferty and Ruff, 1994; Scherf et al., 2013; Kivell et al., 2018), while
84 others are more ambiguous (Ryan and Walker, 2010; Ryan and Shaw, 2012). Other studies
85 focused on the capitate and third metacarpal of African apes concluded that changes in
86 trabecular structure reflected changes in locomotor frequencies throughout ontogeny (Ragni,
87 2020), while additional studies of the capitate x found that capitate trabecular patterns in
88 African apes differed from the Asian apes in relation to their particular locomotor behaviour
89 (i.e., knuckle-walking; Bird et al., 2021); however, to date, no study has focused on the distal

90 humerus in spite of its significance (and of the elbow in general) to forelimb posture and
91 loading during locomotion.

92 The locomotor and postural repertoire of the African apes has been extensively
93 studied (e.g., Inouye, 1994; Inouye, 1992; Doran, 1997; Isler, 2005; Neufuss et al., 2017;
94 Finestone et al., 2018; Thompson et al., 2020). African apes are the most terrestrial of the
95 non-human apes, with gorillas being more terrestrial than chimpanzees in adulthood (Hunt,
96 1991; Doran, 1993; Doran, 1996; Crompton et al., 2010). Additional variation in
97 terrestriality exists within species of chimpanzees and gorilla (e.g., mountain gorillas are
98 more terrestrial than western lowland gorillas; Doran, 1993; Inouye, 1993; Remis, 1994).
99 There are also postural differences in African ape knuckle-walking such that gorillas
100 typically use a pronated hand posture (palm facing backwards), while chimpanzees are more
101 variable but most often use a palm-in posture (Tuttle, 1969; Wunderlich and Jungers, 2009;
102 Matarazzo, 2013; but see Thompson et al., 2020). In addition to knuckle-walking, African
103 apes also use a large diversity of other locomotor behaviours, including vertical climbing,
104 clambering, and suspension (Hunt, 1991; Doran, 1993; Remis, 1994; Crompton et al., 2010).
105 These arboreal behaviours are more frequent during early ontogeny (i.e., <5 years of age) in
106 both chimpanzees and gorillas (Doran, 1997).

107 To investigate the potential knuckle-walking signals in humeral trabecular bone, we
108 compare African apes to the more suspensory Asian apes (orang-utans and hylobatids), semi-
109 suspensory spider monkeys, and both arboreal and terrestrial quadrupedal monkeys (howler
110 monkeys and long-tailed macaques, and Hamadryas baboons, respectively) that vary in both
111 their locomotor behaviours and habitual elbow postures (see below).

112 *Elbow joint loading predictions*

113 The main movement of the primate elbow is flexion-extension, the range of which is
114 mostly determined by the shape of the olecranon process of the ulna (Harrison, 1982). Apes

115 have a short olecranon processes that allows full (and even hyper-) extension of the elbow,
116 whereas monkeys have a long olecranon process that impedes full extension at the elbow
117 when it articulates with the olecranon fossa of the humerus. Stabilisation of the ape elbow is
118 achieved in part by a keeled humeroulnar joint. In apes, the humeral trochlea has a medial
119 and lateral keel (creating the spool-shape), in which the medial keel, particularly in monkeys,
120 helps to resist mediolateral forces generated by the elbow and digit extensors that threaten to
121 rotate and displace the ulna medially (Preuschoft, 1973; Schmitt, 2003; Hunt, 2016). The
122 median keel in the trochlear notch of the ulna further enhances mediolateral stabilization.
123 Apes have a round radial head that articulates with a globular capitulum and deep zona
124 conoidea (an indentation between the lateral keel and the capitulum) of the distal humerus,
125 which provides greater stabilization of the radiohumeral joint in all positions of
126 pronosupination (although pronosupination itself occurs at proximal and distal radioulnar
127 joints) and stabilizes the radial head during the movement. Habitual elbow postures during
128 locomotion can include full (or hyper-) extension, full flexion, or a variety of postures
129 involving semi-flexion of the elbow (Rose, 1988). While elbow joint angle can be measured
130 directly, it is not possible to directly quantify joint reaction forces (loading). However,
131 relative loading conditions (e.g., higher loads on one region of the joint) can be reasonably
132 predicted given variation in anatomy and joint posture.

133 Therefore, we predict that an elbow habitually loaded in (1) **extension** (~180°) will
134 result in a distal humerus showing a relatively high density of trabeculae (bone volume
135 fraction, bone volume/total volume [BV/TV]) concentrated in the distal and/or posterior
136 aspects of the trochlea and the distal capitulum, while **hyperextension** (>180°) might be
137 reflected in higher BV/TV in the posterior aspect of the trochlea as the olecranon impinges
138 into the humerus' fossa; (2) **semi-flexion** (>90° and <180°) will result in a distal humerus
139 showing high BV/TV concentrated more anterodistally in the capitulum and trochlea, and

140 potentially the medial keel of the trochlea, which resists the medial forces of the muscles
141 acting at the elbow; (3) **flexion** ($\leq 90^\circ$) will result in a distal humerus showing high BV/TV
142 concentrated only in the anterior regions of the capitulum and trochlea.

143 Based on the model above, we make the following predictions for habitual loading of
144 the elbow of African apes, Asian apes and non-hominoid taxa studied:

145 Gorillas and chimpanzees The elbow is generally held in an extended posture during
146 knuckle-walking in all African apes during stance phase (Zylstra, 1999; Hunt, 1996). The
147 mean elbow joint angle of gorillas (*Gorilla*) is closer to 180 degrees (i.e., fully extended) at
148 midstance than chimpanzees (*Pan*), which display more variability (Isler, 2005; Finestone et
149 al., 2018; Thompson et al., 2020); however, both taxa occasionally use hyperextended elbow
150 postures (Inouye, 1994; Zylstra, 1999; Finestone et al., 2018). As such, we predict that
151 African apes will show a trabecular pattern consistent with habitual loading of a relatively
152 extended elbow during knuckle-walking.

153 Siamangs and orang-utans Orang-utans (*Pongo*) engage most frequently in torso-
154 orthograde suspension, such that the torso is vertically oriented with the hands and feet
155 bearing weight typically in tension with the elbow extended, while during vertical
156 climbing/descent, the elbow is most often flexed (Thorpe and Crompton, 2005; Thorpe and
157 Crompton, 2006; Thorpe et al., 2009). Hylobatids prefer to move through the canopy using
158 brachiation, including ricochet brachiation, as the primary form of locomotion (Hunt, 1991)
159 in which the elbow of the support limb is extended (Swartz, 1989; Swartz et al., 1989). We
160 include siamangs (*Symphalangus*) in our sample whose positional behaviour is more similar
161 to that of orangutans than other hylobatids, likely due to their larger body size (Hunt, 2016).
162 Thus, the expected pattern for the more suspensory Asian apes is habitual loading of an
163 extended elbow. However, if found, we expect potential variation in BV/TV values between
164 the African versus Asian ape extended-elbow trabecular pattern given that African apes more

165 frequently load their forelimb in compression (higher BV/TV) and the Asian apes in tension
166 (lower BV/TV) (Swartz et al., 1989). Additionally, due to their more varied locomotor
167 regimes, orang-utans may alternatively show a more diffuse or unspecific trabecular pattern
168 consistent with an elbow loaded in a variety of different postures.

169 Pronograde monkeys Howler monkeys (*Alouatta* sp.), macaques (*Macaca*
170 *fascicularis*), and baboons (*Papio hamadryas*), most often engage in pronograde
171 quadrupedalism either in the trees (*Alouatta* sp., *M. fascicularis*) or almost exclusively on the
172 ground (*P. hamadryas*) (Cant, 1986; Cant, 1988; Schmidt, 2011). During quadrupedal
173 walking and running the elbow is most often semi-flexed during stance phase (Larney and
174 Larson 2004; Youlatos, 2008) and we predict that quadrupedal monkeys will show a
175 trabecular pattern consistent with a habitually semi-flexed or flexed elbow that primarily
176 incurs load in the parasagittal plane. Spider monkeys most frequently engage in arboreal
177 quadrupedalism but also use semi-brachiation with the aid of a prehensile tail and the elbow
178 is used in extended and semi-flexed postures (Schmitt et al., 2005; Youlatos, 2008). Thus, it
179 is reasonable to predict that spider monkeys may converge with orang-utans in showing a
180 trabecular pattern consistent with an elbow loaded in a variety of different postures due to
181 their more varied locomotor regime.

182

183 **Materials and Methods**

184 The sample used in this study (see Table 1 for details) includes (1) apes: chimpanzees,
185 Virunga mountain gorillas, western lowland gorillas, orang-utans, and siamangs; (2) Old
186 World monkeys: long-tailed macaques and hamadryas baboons; and (3) New World
187 monkeys: howler monkeys and spider monkeys. All individuals were wild-shot adults and
188 showed no obvious signs of pathology.

189 Specimens were scanned using a BIR ACTIS 225/300 industrial microCT scanner
190 (Department of Human Evolution, Max Planck Institute for Evolutionary Anthropology,
191 Germany) and two Nikon XT H 225 ST microCT scanner (Cambridge Biotomography
192 Centre, Department of Zoology, University of Cambridge, UK and Shared Materials
193 Instrumentation Facility, Duke University, USA). The isotropic voxel size range for the
194 sample is 21.9–99.9 μm (Table 1). Scan parameters were 100–160 kV and 100–140 μA ,
195 using a brass or copper filter of 0.2–0.5 mm. All scans were reconstructed as 16-bit TIFF
196 image stacks.

197 All scans were oriented to a homologous position in AVIZO 6.3[®] (Visualization
198 Sciences Group, SAS) and cropped at the end of the medial and lateral ridges, which marks
199 the start of the humeral shaft and the most proximal extent of trabecular bone (SI Fig. S1,
200 S2). All data were segmented using the Ray Casting Algorithm (Scherf and Tilgner, 2009).

201 Medtool 4.2 (www.dr-pahr.at) was used to quantify trabecular bone throughout the
202 distal epiphysis of the humerus using a Holistic Morphometric Analysis (HMA) following
203 the methods described in Gross et al. (2014) and Tsegai et al. (2013). Briefly, cortical bone is
204 separated from the trabeculae (SI Fig. S2) by casting rays at different angles from the outer
205 cortical shell and terminating them on contact with background voxels. The inner structure is
206 then closed with a spherical kernel the size of the average trabecular thickness in that bone
207 (Pahr and Zysset, 2009), and the 3D edge of this inner structure defines the boundary
208 between subchondral trabecular and cortical bone (Gross et al., 2014).

209 Bone volume fraction (BV/TV), quantified as a ratio of bone volume to total volume,
210 and degree of anisotropy (DA), quantified following the mean intercept length (MIL) method
211 and bounded between 0 (isotropy) and 1 (anisotropy), were measured throughout the distal
212 epiphysis using a sampling sphere with a 5-mm diameter on a 2.5- mm background grid.

213 Regions with marked concavities, such as the olecranon fossa, were defined with a bounding

214 box and a correction filter was applied, following Georgiou et al. (2018). An additional
215 protocol was followed to quantify the BV/TV and DA values in the trochlea and capitulum
216 separately, given the complexity of the distal humeral morphology (see SI Fig. S1 for
217 details).

218

219 *Statistical analyses*

220 Descriptive statistics were conducted for BV/TV and DA values for the whole
221 epiphysis, capitulum and trochlea for each genus (SI Table S1; BV/TV and DA individual
222 values can be found in SI Data S1). We tested differences between gorillas and chimpanzees
223 with Mann-Whitney U-tests given their larger sample sizes ($n=7$) (see also SI Appendix S1).
224 However, sample sizes for the comparative taxa were too small (ranging $n=2-4$) to apply
225 probability-based statistical tests (but see SI Appendix S1). Box-and-whisker plots for
226 BV/TV and DA values for the whole epiphysis (Fig. 2), capitulum and trochlea (SI Fig S3)
227 were used instead to evaluate and compare trabecular parameters across taxa. All statistical
228 tests were done in R v.3.6.1 (R Core Team) using the ‘dyplr’ package (Wickham et al.,
229 2018). A bivariate plot of mean DA and BV/TV for all specimens in the sample was
230 generated in R to explore the relationship between BV/TV, DA and the distribution of groups
231 in relation to these two parameters (Fig. 3).

232 Finally, allometry was investigated by means of linear regression of log transformed
233 variables following Jungers (1991). We obtained the average humeral head diameter (linear
234 dimension 2: mean of two chords perpendicular to greater and lesser tubercles; Jungers,
235 1991: 392) and log-transformed them with natural logarithms (\ln). The result was used as an
236 independent variable of body size (SI Dataset S1). We also applied natural logarithms to the
237 BV/TV and DA values of each individual for the whole epiphysis, and obtained the linear
238 regression models between these dependent variables and body size (SI Table S2).

239

240 *Qualitative analyses*

241 Three-dimensional tetrahedral meshes with a 1-mm mesh size were created using
242 CGAL 4.4 (CGAL, Computational Geometry; <http://www.cgal.org>) and BV/TV values were
243 interpolated from the background grid onto the elements creating BV/TV distribution colour
244 maps. Internal BV/TV distribution was visualised in Paraview (Ahrens et al., 2005).

245

246 **Results**

247 Colour maps of BV/TV for all individuals in all taxonomic groups in the sample are
248 presented in the SI Fig. S3, with one representative specimen in Fig. 1. Variation in the
249 distribution of trabeculae in the distal humerus is described below in detail.

250 Chimpanzees (*P. t. verus*) All chimpanzees display a very similar pattern in BV/TV
251 distribution (SI Fig. S3). High BV/TV values are concentrated anteriorly on the capitulum
252 and anteriorly, distally and posteriorly on the trochlea, with the highest values typically
253 located on the medial keel of the trochlea. All individuals have relatively high BV/TV
254 distribution throughout the articular surfaces of the distal humerus compared with other taxa.
255 Both epicondyles show high BV/TV with the medial epicondyle generally exhibiting
256 markedly higher BV/TV than that of the lateral epicondyle.

257 Western lowland gorillas (*G. g. gorilla*) For the western lowland gorillas, three out of
258 four individuals display high BV/TV on the disto-posterior trochlea and slightly less on the
259 capitulum (SI Fig. S3). There are small areas of high BV/TV in the medial epicondyle,
260 situated distally to the medial ridge, but notably low BV/TV in the lateral epicondyle. The
261 fourth individual (PC M29) displays exceptionally high BV/TV throughout the distal
262 humerus, and particularly at both the distal trochlea and the anterior capitulum.

263 Mountain gorillas (*G. b. beringei*) All mountain gorillas present a pattern that is
264 distinct from that of lowland gorillas. There is high BV/TV on the antero-distal capitulum as
265 well as the anterior portion of both the medial and lateral trochlear keels that extend distally
266 and posteriorly with minimal connection. Mountain gorillas show high BV/TV at both
267 epicondyles, with higher concentrations in the medial epicondyle and in the posterior aspect
268 of the lateral epicondyle, expanding into the lateral crest, with the exception of one individual
269 (GP 78; SI Fig. S3).

270 Asian apes In both suspensory orang-utans (*P. pygmaeus*) and siamangs (*S.*
271 *syndactylus*), high BV/TV is mainly concentrated on the distal and posterior trochlea. There
272 are two exceptions to this pattern: one orang-utan (ZMS 1982-0092), which shows high
273 BV/TV throughout the epiphysis, and particularly at the epicondyles and the medial trochlear
274 keel, and one siamang (ZMB 38573), which shows high BV/TV at the anterior capitulum, the
275 distal and posterior trochlea, and the medial epicondyle (SI Fig. S3). Overall, both taxa show
276 low or very low BV/TV in the medial and lateral epicondyles.

277 Monkeys Pronograde quadrupedal monkeys (macaques, baboons, howler monkeys) as
278 well as spider monkeys with a more varied locomotor repertoire, all display a common
279 pattern of high BV/TV throughout the epiphysis. On the trochlea, BV/TV is concentrated
280 anteriorly as well as distally, while it is distally and anteriorly concentrated on the capitulum.
281 Howler monkeys display higher BV/TV in the capitulum than spider monkeys, while
282 baboons and macaques display higher BV/TV throughout the distal humerus relative to all
283 the other taxa in our sample (SI Fig. S3). Monkeys generally have relatively lower BV/TV in
284 the epicondyles compared with apes, however, some individuals (ZMB 44814, ZMB 35764,
285 ZMB 48496) show slightly higher BV/TV values in the medial epicondyle.

286 Despite these qualitative differences in BV/TV distribution, two-tailed Mann-Whitney
287 *U*-tests reveal no significant differences between chimpanzees and gorillas in BV/TV ($p =$

288 0.165), or separately for the capitulum ($p = 0.710$) and trochlea ($p = 0.535$). Although small
289 sample sizes prohibited statistical testing among the rest of the sample, box-and-whisker plots
290 reveal that baboons consistently showed the highest BV/TV for the whole epiphysis,
291 capitulum and trochlea, followed closely by gorillas and then chimpanzees. In contrast,
292 atelines (howler and spider monkeys) and macaques consistently showed the lowest BV/TV
293 for each region (Fig. 2; SI Fig. S3).

294 Degree of anisotropy (DA) colour maps (Fig. 1) do not reveal clear regional
295 interspecific differences that can be readily associated to locomotor behaviour. However, the
296 Mann-Whitney U -tests found significant differences in DA between African apes, with
297 chimpanzees showing higher DA values than gorillas for the whole epiphysis ($p = 0.002$),
298 capitulum ($p = 0.038$) and trochlea ($p = 0.038$). Box-and-whisker plots reveal that
299 chimpanzees and baboons display the highest DA for each region, whereas gorillas show
300 relatively low DA (albeit, with a wide range of variation), similar to those of siamangs,
301 atelines and macaques. Orang-utans display the greatest variation in DA values for each
302 region.

303 A bivariate plot of BV/TV and DA (Fig. 3) distinguishes siamangs, atelines and
304 macaques from the remainder of the sample with relatively low BV/TV and DA. Great apes
305 and baboons generally have higher BV/TV values, but as a group are more variable in their
306 DA values.

307 The linear regressions between our proxy for body size and BV/TV is significant ($p =$
308 <0.000) but the R^2 and adjusted R^2 values are not very high ($R^2 = 0.61$, $_{Adj}R^2 = 0.60$) (SI
309 Table S2). The linear regression between body size and DA is not significant ($p = 0.058$, $R^2 =$
310 0.11 , $_{Adj}R^2 = 0.08$).

311

312 **Discussion**

313 This study found that trabecular bone holds functional signals of variation in elbow
314 joint loading that are consistent with differences between taxa that more often use a semi-
315 flexed elbow posture during locomotion compared with those that use an extended elbow
316 posture. Importantly, most individuals across our entire sample showed relatively high
317 BV/TV at the medial epicondyle, which likely reflects the high loading incurred by
318 antebrachial flexor muscles, highlighting the importance of internal muscle forces on bone
319 modelling (which can be up to seven times higher than external reaction forces; e.g.,
320 Preuschoft, 1973). We found a significant but weak allometric relationship between body size
321 and BV/TV in our sample; the low R^2 and $\Delta_{adj}R^2$ indicate that other factors explain the BV/TV
322 patterns found here beside body size (Bird et al., 2021) BV/TV (together with DA, which
323 was not significantly associated with body size in our sample) determines most of the
324 mechanical stiffness of trabecular bone (Maquer et al., 2015), with the underlying assumption
325 that higher BV/TV reflects higher habitual mechanical loading. Based on previous studies
326 (e.g. Doube et al., 2011; Barak et al., 2013) and given that BV/TV values inherently account
327 for variation in size (i.e. as a ratio), our finding that BV/TV is at least partially influenced by
328 body size was unexpected. However, given our sample sizes are relatively small (more so for
329 the comparative sample than for *Pan* and *Gorilla*), further studies are needed to explore the
330 allometric influence on BV/TV in the distal humerus within species and how this might differ
331 from other skeletal regions. Finally, some specimens display sections of compact cortical
332 bone (e.g., in specimen ZMB 44079 (*Ateles*), the crest arising from the medial epicondyle)
333 which may be replacing trabecular bone; the biomechanical information and potential bias
334 this might introduce should be further explored in relation to trabecular bone patterns and
335 locomotor behaviours in the distal humerus in the future.

336 Old and New World monkeys, chimpanzees, and, slightly less evidently, mountain
337 gorillas showed a semi-flexed elbow pattern. The BV/TV distribution pattern on the articular

338 surfaces of the trochlea and capitulum they exhibited included high BV/TV anteriorly in the
339 capitulum that merged with regions of high BV/TV on the trochlea, which expanded
340 anteriorly, distally and posteriorly. The highest BV/TV concentration for the semi-flexed
341 elbow pattern was found in the medial keel of the trochlea. Thus, the BV/TV pattern found
342 for the pronograde quadrupeds (macaques, baboons and howler monkeys) was consistent
343 with our predictions. In the semi-flexed elbow joint posture during stance phase of
344 quadrupedal gait, there is increased contact at the humeroradial joint (Rose, 1988). This is
345 consistent with the anterodistally high BV/TV values in the capitulum in these taxa. High
346 BV/TV across the trochlea in general, with particularly high BV/TV at the medial keel, is
347 consistent with the medially-directed, compressive forces exerted by the forearm flexor
348 muscles (Preuschoft, 1973; Hunt, 2016) and the subsequent mediolateral substrate reaction
349 forces (which are greater during terrestrial locomotion than on arboreal substrates) trying to
350 displace the ulna medially (Schmitt, 2003).

351 Spider monkeys are substantially less quadrupedal than the other monkeys in our
352 sample, but contrary to our predictions, they aligned with the semi-flexed elbow trabecular
353 pattern. Nevertheless, this is consistent with their most frequent locomotor behaviour,
354 quadrupedal walking and running, which they may engage in over 50% of their locomotor
355 time, depending on the species (Youlatos, 2008). Spider monkeys only engage in suspensory
356 behaviours ~25% of time (Cant, 1986) and use their prehensile tails (and occasionally their
357 feet) for support. As such, their forelimbs do not always support full body weight during
358 suspension as in hylobatids and orang-utans (Swartz et al., 1989; Youlatos, 2008). Moreover,
359 during tail-assisted suspension, the trailing limb elbow is oftentimes held in a semi-flexed
360 position at the beginning of a swing (Youlatos, 2008), which is consistent with the trabecular
361 pattern observed.

362 Baboons are the most terrestrial taxon among our sample (Schmidt, 2011) and their
363 high DA values are consistent with a joint loaded in a highly stereotypical manner (Tsegai et
364 al., 2013), facilitated by a limb joint morphology advantageous for movement in the
365 parasagittal plane (Rose, 1988). The comparatively lower DA values in macaques and
366 atelines, in contrast, may reflect a greater range of movement needed to navigate an arboreal
367 environment.

368 Orang-utans, siamangs and western lowland gorillas each showed an extended-elbow
369 pattern, consisting of low BV/TV in the capitulum coupled with high BV/TV in the trochlea,
370 where it was mostly restricted to its distal and posterior aspects. The shared pattern of
371 siamangs and orang-utans (African apes will be discussed separately below) is consistent
372 with an extended-elbow position during brachiation and torso-orthograde suspension, and
373 also consistent with our predictions. The forelimb of brachiating gibbons and, presumably,
374 siamangs experiences maximum strain at the extended-elbow midsupport phase of the swing,
375 as the animal reaches the bottom of the brachiating arc, with the humerus experiencing tensile
376 loading (Swartz, 1989; Swartz et al., 1989). The slightly lower BV/TV values in Asian apes
377 relative to gorillas may reflect this tensile loading compared to compressive loading of an
378 extended elbow in gorillas (see below). The relatively low DA values of siamangs are also
379 consistent with highly mobile joints. In contrast, orang-utans displayed extremely variable
380 (including the lowest and highest in the sample) DA values. High intraspecific variability in
381 orang-utan trabecular structure, including DA, has also been found in the distal femur
382 (Georgiou et al., 2018) and capitate (Bird et al., 2020).

383 We predicted that African great apes would share the same extended (or near-
384 extended)-elbow pattern that is typically described for knuckle-walking (Tuttle, 1969;
385 Inouye, 1993; Zylstra, 1999; Finestone et al., 2018). Our results did not fully support this
386 prediction. Instead, chimpanzees (and to a lesser extent, mountain gorillas, discussed

387 separately below) presented a flexed-elbow BV/TV pattern similar to the monkeys. Recent
388 studies (Finestone et al., 2018; Thompson et al., 2020) have demonstrated that there is more
389 variability in chimpanzee elbow joint kinematics during knuckle-walking than previously
390 understood, which could explain the flexed-elbow pattern of chimpanzees found in our study.
391 Our results suggest that chimpanzees load their elbow differently from that of gorillas, with a
392 more flexed posture (Inouye, 1993; Zylstra, 1999; Finestone et al., 2018), which has been
393 observed in captive chimpanzees (A.Z. unpublished research). It should be noted that our
394 sample consists of Tai chimpanzees, one the most arboreal and acrobatic chimpanzee groups
395 (Doran, 1994), and the flexed-elbow trabecular pattern may alternatively reflect a bony
396 response to the stresses of arboreal behaviours, such as vertical climbing or clambering
397 (Doran, 1996). Although we have found clear patterns of flexed vs. extended elbow postures
398 in relation to habitual behaviour in the other taxa studied, other species and subspecies of
399 chimpanzee such as bonobos or East African chimpanzees (*P. paniscus* and *P. troglodytes*
400 *schweinfurthii*, respectively, which, unfortunately, were not available for this study) with
401 different ecolocomotor characteristics should be studied to see if they also demonstrate a
402 flexed-elbow trabecular pattern.

403 In comparison to chimpanzees, western lowland gorillas generally exhibited a BV/TV
404 distribution pattern similar to that of suspensory Asian apes, and consistent with habitual
405 loading in an extended-elbow joint posture (albeit, with the stated difference in loading
406 regimes, i.e., compression vs. tension respectively; Swartz et al., 1989). Our African ape
407 sample is skewed towards females, which display different frequencies of locomotor
408 behaviours with respect to their males counterparts (Inouye, 1994; Doran, 1996; Doran,
409 1997). Owing to their dense-canopy environment, all western lowland gorillas, including
410 large males, spend up to a 35% of their time in trees, even in adulthood (Ruff et al., 2018 and
411 references therein), but the likelihood of the extended-elbow pattern being related to a more

412 suspensory behaviour is low, since lowland gorillas and chimpanzees engage in roughly the
413 same, almost negligible amount of suspensory locomotion, ranging from less than 1% to
414 3.6% of their locomotor time (Crompton et al., 2010). If western lowland gorillas follow a
415 similar pattern to mountain gorillas, then they most often vertically climb with an extended
416 elbow only on large or extra-large diameter substrates (Neufuss et al., 2017). In addition,
417 gorillas display an elbow morphology (i.e., generally flatter joints; Rose, 1993) that are
418 advantageous for coping with loads incurred during terrestrial locomotion with an extended
419 forearm. Finestone et al. (2018) showed that, although there is general similarity in knuckle-
420 walking kinematic pattern in both captive chimpanzees and lowland gorillas, gorillas used a
421 slightly more (but not significantly so) extended elbow posture at midstance. Although it is
422 uncertain how less frequent, but potentially higher loading, behaviours may drive modelling
423 of the trabeculae (e.g., Umemura, 2002), the trabecular pattern in lowland gorillas (as well as
424 in chimpanzees) most likely reflects posture and load during knuckle-walking over any other
425 behaviour, as previously found for other forelimb structures, e.g., capitate and third
426 metacarpal (Ragni, 2020) and the capitate (Bird et al., 2021).

427 Surprisingly, mountain gorillas displayed a BV/TV distribution pattern that was
428 intermediate between the extended-elbow posture of western lowland gorillas and the flexed-
429 elbow posture of chimpanzees. Mountain gorillas had high BV/TV at the anterior capitulum
430 and at both trochlear keels, but without the high BV/TV throughout the distal humerus found
431 in chimpanzees and monkeys. Mountain gorillas are the most terrestrial of all *Gorilla* species
432 (and apes, in general) due to their montane forest habitat (Tocheri et al., 2011; Jabbour and
433 Pearman, 2016; Ruff et al., 2018). Analyses of forelimb diaphyseal strength proportions show
434 mountain gorillas have stronger ulnae with respect to radii (Ruff et al., 2018), possibly due
435 their high humeral torsion (greater than in any other ape; Inouye, 1993) and a more pronated
436 hand during knuckle-walking, which leads to more load being transferred through the ulna.

437 Mountain gorillas have shorter fingers than their western counterparts, and, while knuckle-
438 walking kinematics of mountain gorillas have not yet been studied, Thompson et al. (2020)
439 documented a surprising amount of variability in the hand postures used during terrestrial
440 locomotion, in which 40% of the hand postures included fist-walking, loading of the dorsal
441 metacarpus or modified palmigrady. More data on elbow joint kinematics in African apes is
442 needed to fully ascertain whether mountain gorillas use and load their forelimb differently
443 from that of western lowland gorillas during knuckle-walking and in a way that is more
444 similar biomechanically at the elbow to that of chimpanzees. Furthermore, the mountain
445 gorillas in our sample displayed high variability in both BV/TV values and distribution, and
446 thus future studies incorporating larger samples in comparison to other apes would be able to
447 reveal the potential functional significance of this intraspecific variability.

448 Further trabecular differences between gorillas (including mountain gorillas) and
449 chimpanzees were found in DA values. Chimpanzees exhibited significantly higher DA than
450 gorillas, which was not expected given the generally higher amount of arboreal locomotion
451 and, presumably, more varied joint loading at the elbow in chimpanzees. Although the
452 variability in mountain gorilla hand postures noted above (Thompson et al., 2020) may partly
453 explain lower DA in this taxon, we suggest that generally low DA in gorillas might also
454 reflect a different bone functional adaptation response within the trabecular structure.
455 Gorillas might offset the need of highly aligned trabeculae (i.e., high DA) to diffuse the
456 incurred stress acting on the distal humerus by possessing thicker trabecular struts, as is
457 suggested might be the case in their distal femur (Georgiou et al., 2018). Future investigation
458 of additional trabecular parameters, including trabecular thickness and separation, are needed
459 to test this hypothesis.

460 The resolution of the functional signal in the distal humerus did not differentiate each
461 locomotor behaviour but did provide a clear distinction between a flexed-elbow *versus* an

462 extended-elbow posture that is generally consistent with the most frequent locomotor
463 behaviours. Moreover, inferred joint posture and loading differences found between
464 chimpanzees and gorillas, and between gorilla species, pinpoint possible divergent
465 biomechanical strategies adopted by African apes during knuckle-walking (Kivell and Smith,
466 2009; Ragni, 2020). More studies are needed to better understand potential variation in
467 knuckle-walking and its evolution; however, differences revealed by trabecular structure
468 within African apes add further evidence to the hypothesis that knuckle-walking is not a
469 unified biomechanical phenomenon (Dainton and Macho, 1999; Kivell and Schmitt, 2009;
470 Hunt, 2016) with potential bearing on the role knuckle-walking played, if any, in the origin(s)
471 of hominin bipedalism.

472

473 **Acknowledgements**

474 We are grateful to S. McFarlin for facilitating access to and scanning the Virunga
475 mountain gorilla specimens, the Rwandan government for permission to study skeletal
476 remains curated by the Mountain Gorilla Skeletal Project (MGSP) established through the
477 Rwanda Development Board's Department of Tourism and Conservation, Dian Fossey
478 Gorilla Fund International, Gorilla Doctors, Institute of National Museums of Rwanda, The
479 George Washington University, and New York University College of Dentistry, and funded
480 by the National Science Foundation (BCS-0852866, BCS-0964944, BCS-1520221), National
481 Geographic Society's Committee for Research and Exploration (8486-08), and The Leakey
482 Foundation. Scanning of the mountain gorilla specimens was funded by the National Science
483 Foundation (BCS 1517561). We also thank the following curators and their institutions for
484 access to specimens in their care: I. Livne, Powell-Cotton Museum (Birchington, UK); A.
485 van Heteren and M. Hiermeier, Zoologische Staatssammlung München (Munich, Germany);
486 F. Mayer and C. Funk, Museum für Naturkunde – Leibniz Institute for Evolution and

487 Biodiversity Science (Berlin, Germany). We thank D. Plotzki (MPI-EVA) and K. Smithson
488 (Cambridge Biotomography Centre) for scanning assistance, C. Dunmore and L. Georgiou
489 for help with analyses, and M. Skinner and C. Dunmore for their comments on earlier
490 versions of the manuscript. This research is supported by the European Commission's
491 Horizon 2020 Marie Skłodowska-Curie Individual Fellowship Programme (H2020-MSCA-
492 IF-2015, grant 703608 to JAM) and ERC Starting Grant 336301 (TLK), and the Agència de
493 Gestió d'Ajust Universitaris i de Recerca of the Generalitat de Catalunya (Beatriu de Pinós
494 BP0058–H2020 MSCA-Cofund, grant 801370 to JAM). We would also like to thank the
495 Editor (M. Zelditch), Associate Editor (J. Day), A. Houssaye and an anonymous reviewer for
496 their comments which helped improve an earlier version of this manuscript.

497

498 **Ethics statement**

499 All methods were carried out in accordance with the University of Kent ethical
500 guidelines and were approved by both the University of Kent and the Institut Català de
501 Paleontologia Ethics Committee.

502

503 **Author contributions**

504 JAM and TLK designed the research, JAM and AZ acquired the data, JAM performed
505 the analyses, and JAM, TLK and AZ interpreted the data, JAM wrote the manuscript. All
506 authors reviewed the manuscript.

507

508 **Competing interests**

509 The author(s) declare no competing interests.

510

511 **Data availability**

512 All data analysed can be found as a csv dataset in Dryad:

513 <https://doi.org/10.5061/dryad.9ghx3ffhz>

514

515 **References**

516

517 Ahrens, J., Geveci, B., & Law, C. Paraview: An end-user tool for large data visualization. In:
518 Hansen, C. D., Johnson, C. R, editors. The visualization handbook. New York:
519 Elsevier. pp. 717–731.

520 Barak, M. M., Lieberman, D. D., Hublin. J.-J. 2011. A Wolff in sheep’s clothing: Trabecular
521 bone adaptation in response to changes in joint loading orientation. *Bone* 49: 1141–
522 1151.

523 Barak, M.M., Lieberman, D.E., Hublin, J-J. 2013. Of mice, rats and men: trabecular bone
524 architecture in mammals scales to body mass with negative allometry. *J. Struct. Biol.*
525 183: 123–131.

526 Begun, D. R. 1992. Miocene fossil hominids and the chimp-human clade. *Science* 257:
527 1929–1933.

528 Biewener, A. A., Fazzalari, N. L., Konieczynski, D. D., Baudinette, R. V. 1996. Adaptive
529 changes in trabecular architecture in relation to functional strain patterns and disuse.
530 *Bone* 19: 1–8.

531 Bird, E. E., Kivell, T. L., Skinner, M. M. Cortical and trabecular bone structure of the
532 hominoid capitate. *J. Anat.* 239: 351–373.

533 Cant, J.G.H. 1988. Positional behavior of long-tailed Macaques (*Macaca fascicularis*) in
534 Northern Sumatra. *Am. J. Phys. Anthropol.* 76: 29–37.

535 Cant, J. G. H. 1986. Locomotion and feeding postures of Spider and Howling monkeys: Field
536 study and evolutionary interpretation. *Folia Prim.* 46: 1–14.

537 Crompton, R. H., Sellers, W. I., Thorpe, S. K. S. 2010. Arboreality, terrestriality and
538 bipedalism. *Phil. Trans. R. Soc. B* 365: 3301–3314.

539 Dainton, M., Macho, G. A. 1999. Did knuckle walking evolve twice? *J. Hum. Evol.* 36: 171–
540 194.

541 Doran, D. M. 1993. Comparative locomotor behavior of chimpanzees and bonobos: the
542 influence of morphology on locomotion. *Am. J. Phys. Anthropol.* 91: 83–98.

543 Doran, D. M. 1996. Comparative positional behavior of the African apes. In: McGrew, M. C.,
544 Marchant, L. F., & Nishida, T., editors. *Great ape societies*. Cambridge: Cambridge
545 University Press. pp. 213–224.

546 Doran, D. M. 1997. Ontogeny of locomotion in mountain gorillas and chimpanzees. *J. Hum.*
547 *Evol.* 32: 323–344 (1997).

548 Doran, D. M., Hunt, K. D. 1994. Comparative locomotor behavior of chimpanzees and
549 bonobos. In: Wrangham, R. W., McGrew, W. C., De Waal, F., editors. *Chimpanzee*
550 *cultures*. Chicago: Chicago Academy of Sciences. pp. 93-108.

551 Doube, M., Klosowski, M.M., Wiktorowicz-Conroy, A.M., Hutchinson, J.R., Shefelbines, J.
552 2011. Trabecular bone scales allometrically in mammals and birds. *Proc Royal Soc B*
553 278: 3067–3073.

554 Drapeau, M. S. M. 2008. Articular morphology of the proximal ulna in extant and fossil
555 hominoids and hominins. *J. Hum. Evol.* 55: 86–102.

556 Finestone, E. M., Brown, M. H., Ross, S. R., Pontzer, H. 2018. Great ape walking
557 kinematics: Implications for hominoid evolution. *Am. J. Phys. Anthropol.* 166: 43–
558 55.

559 Georgiou, L., Kivell, T. L., Pahr, D. H., Skinner, M. M. 2018. Trabecular bone patterning in
560 the hominoid distal femur. *PeerJ* 6: e5156.

561 Gross, T., Kivell, T. L., Skinner, M. M., Nguyen, N. H., Pahr, D. H. 2014. A CT-image-based
562 framework for the holistic analysis of cortical and trabecular bone morphology.
563 *Palaeontol. Electron.* 17: 1–13.

564 Harrison, T. 1982. Small bodied apes from the Miocene of East Africa. Doctoral dissertation,
565 University College London.

566 Hunt, K.D. 1991. Positional behavior in the Hominoidea. *Int. J. Primatol.* 12: 95–118.

567 Hunt, K.D. 2016. Why are there apes? Evidence for the co-evolution of ape and monkey
568 ecomorphology. *J. Anat.* 228: 630–685.

569 Hunt, K.D., Cant, J. G. H., Gebo, D. L., Rose, M. D., Walker, S. E., Youlatos, D. 1996.
570 Standardized descriptions of primate locomotor and postural modes. *Primates* 37:
571 363–387.

572 Inouye, S. E. 1992. Ontogeny and allometry of African ape manual rays. *J. Hum. Evol.*, 23:
573 107–138.

574 Inouye, S. E. 1994. The Ontogeny of Knuckle-walking Behavior and Associated Morphology
575 in the African Apes. Doctoral dissertation, Northwestern University.

576 Inouye, S. E. 2003. Intraspecific and ontogenetic variation in the forelimb morphology of
577 Gorilla. In: Taylor, A. B., Goldsmith, M. L., editors. *Gorilla biology: a*
578 *multidisciplinary perspective*. Cambridge: Cambridge University Press. pp. 194–235.

579 Isler, K. 2005. 3D-Kinematics of vertical climbing in hominoids. *Am. J. Phys. Anthropol.*
580 126: 66–81.

581 Jabbour, R. S., Pearman, T. L. 2016. Geographic variation in gorilla limb bones. *J. Hum.*
582 *Evol.* 95: 68–79.

583 Jungers, W. L. 1991. Scaling of postcranial joint size in hominoid primates. *Hum. Evol.* 6:
584 391–399.

585 Khosla, S., Melton, J. L., Achenbach, S. J., Oberg, A., L., Riggs, L. B. 2006. Hormonal and
586 Biochemical Determinants of Trabecular Microstructure at the Ultradistal Radius in
587 Women and Men. *J. Cli. Endocrinol. Metab.* 91: 885–891.

588 Kivell, T.L. 2016. A review of trabecular bone functional adaptation: what have we learned
589 from trabecular analyses in extant hominoids and what can we apply to fossils? J.
590 Anat. 228: 569–594.

591 Kivell, T. L., Davenport, R., Hublin, J.-J., Thackeray, J. F., Skinner, M. M. 2018. Trabecular
592 architecture and joint loading of the proximal humerus in extant hominoids, *Ateles*,
593 and *Australopithecus africanus*. Am. J. Phys. Anthropol. 167: 348–365.

594 Kivell, T. L., Schmitt, D. 2009. Independent evolution of knuckle-walking in African apes
595 shows that humans did not evolve from a knuckle-walking ancestor. Proc. Nat. Acad.
596 Sci. USA 106: 14241–14246.

597 Larney, E., Larson, S. G. 2004. Compliant walking in primates: elbow and knee yield in
598 primates compared to other mammals. Am J. Phys. Anthropol. 125: 42–50.

599 Lieberman, D. E., Devlin, M. J., Pearson, O. M. 2001. Articular area responses to mechanical
600 loading: effects of exercise, age, and skeletal location. Am. J. Phys. Anthropol. 116:
601 266–277.

602 Lovejoy, C. O., Suwa, G., Simpson, S. W., Matternes, J. H., White, T. D. 2009. The great
603 divides: *Ardipithecus ramidus* reveals the postcrania of our last common ancestor
604 with African apes. Science 326: 73–106.

605 Macho, G. A., Abel, R. L., Schutkowski, H. 2005. Age changes in bone microstructure: do
606 they occur uniformly? Int. J. Osteoarchaeol. 15: 421–430.

607 Maquer, G., Musy, S. N., Wandel, J., Gross, T., Zysset, P. K. 2015. Bone volume fraction
608 and fabric anisotropy are better determinants of trabecular bone stiffness than other
609 morphological variables. J. Bone Min. Res. 30: 1000–1008.

610 Matarazzo, S. 2013. Manual pressure distribution patterns of knuckle-walking apes. Am. J.
611 Phys. Anthropol. 152: 44–50.

612 Neufuss, J., Robbins, M. M., Baeumer, J., Humle, T., Kivell, T. L. 2017. Comparison of
613 hand use and forelimb posture during vertical climbing in mountain gorillas (*Gorilla*
614 *beringei beringei*) and chimpanzees (*Pan troglodytes*). *Am. J. Phys. Anthropol.* 164:
615 651–664.

616 Pahr, D. H., Zysset, P. K. 2009. From high-resolution CT data to finite element models:
617 development of an integrated modular framework. *Comput. Met. Biomech. Biomed.*
618 *Eng.* 12: 45–57.

619 Pontzer, H., Lieberman, D. E., Momin, E., Devlin, M. J., Polk, J. D., Hallgrímsson, B.,
620 Cooper, D. M. L. 2006. Trabecular bone in the bird knee responds with high
621 sensitivity to changes in load orientation. *J. Exp. Biol.* 209: 57–65.

622 Preuschoft, H. 1973. The functional anatomy of the upper extremity. In: Bourne, J., editor.
623 *The chimpanzee*, vol 6. Basel: Karger. pp. 34–120.

624 R Core Team. 2019. R: A Language and Environment for Statistical Computing. R
625 Foundation for Statistical Computing. <https://www.r-project.org>.

626 Rafferty, K. L., Ruff, C. B. 1994. Articular structure and function in *Hylobates*, *Colobus*, and
627 *Papio*. *Am. J. Phys. Anthropol.* 94: 395–408.

628 Ragni, A. J. 2020. Trabecular architecture of the capitate and third metacarpal through
629 ontogeny in chimpanzees (*Pan troglodytes*) and gorillas (*Gorilla gorilla*). *J. Hum.*
630 *Evol.* 138: 102702.

631 Remis, M. J. 1994. Feeding ecology and positional behavior of Western gorillas (*Gorilla*
632 *gorilla gorilla*) in the Central African Republic. Doctoral dissertation, Yale
633 University.

634 Richmond, B.G., Begun, D.R., Strait, D.S. 2001. Origin of human bipedalism: The knuckle-
635 walking hypothesis revisited. *Am. J. Phys. Anthropol.* 116: 70–105.

- 636 Richmond, B., Strait, D. 2000. Evidence that humans evolved from a knuckle-walking
637 ancestor. *Nature* 404: 382–385.
- 638 Rose, M. D. 1988. Another look at the anthropoid elbow. *J. Hum. Evol.* 17: 193–224.
- 639 Rose, M. D. 1993. Functional anatomy of the elbow and forearm in primates. In: Gebo, D. L.,
640 editor. *Postcranial adaptations in nonhuman primates*. DeKalb: Northern Illinois
641 University Press. pp. 70–95.
- 642 Ruff, C. B., Burgess, L. M., Junno J.-A., Mudakikwa, A., Zollikofer, C. P., Ponce de León,
643 M., McFarlin, S. C. 2018 . Phylogenetic and environmental effects on limb bone
644 structure in gorillas. *Am. J. Phys. Anthropol.* 166: 353– 372.
- 645 Ryan, T. M., Raichlen, D. A., Gosman, J. H. 2017. Structural and mechanical changes in
646 trabecular bone during early development in the human femur and humerus. In:
647 Percival, C. J., Richtsmeier, J. T. Building, editors. *Bones: Bone Formation and*
648 *Development in Anthropology*. Cambridge: Cambridge University Press. pp. 281–
649 302.
- 650 Ryan, T. M., Shaw, C. N. 2012. Unique suites of trabecular bone features characterize
651 locomotor behavior in human and non-human anthropoid primates. *PLoS ONE* 7:
652 e41037.
- 653 Ryan, T. M., Walker, A. 2010. Trabecular bone structure in the humeral and femoral heads of
654 anthropoid primates. *Anat. Rec.* 293: 719–729.
- 655 Saers, J. P. P., Ryan, T. M., Stock, J. T. 2019. Trabecular bone functional adaptation and
656 sexual dimorphism in the human foot. *Am. J. Phys. Anthropol.* 168: 154–169.
- 657 Scherf, H., Harvati, K., Hublin, J.-J. 2013. A comparison of proximal humeral cancellous
658 bone of great apes and humans. *J. Hum. Evol.* 65: 29–38.

659 Scherf, H., Tilgner, R. 2009. A new high-resolution computed tomography (CT)
660 segmentation method for trabecular bone architectural analysis. *Am. J. Phys.*
661 *Anthropol.* 140: 39–51.

662 Schmidt, M. 2011. Locomotion and postural behaviour. *Adv. Sci. Res.* 5: 23–39.

663 Schmitt, D. 1994. Forelimb mechanics as a function of substrate type during quadrupedalism
664 in two anthropoid primates. *J. Hum. Evol.* 26: 441–457.

665 Schmitt, D. 2003. Mediolateral reaction forces and forelimb anatomy in quadrupedal
666 primates: implications for interpreting locomotor behavior in fossil primates. *J. Hum.*
667 *Evol.* 44: 47–58.

668 Schmitt, D., Rose, M.D., Turnquist, J.E., Lemelin, P. 2005. Role of the prehensile tail during
669 ateline locomotion: Experimental and osteological evidence. *Am. J. Phys. Anthropol.*
670 126: 435–446.

671 Swartz, S.M. 1989. Pendular mechanics and the kinematics and energetics of brachiating
672 locomotion. *Int. J. Primatol.* 10: 387–418.

673 Swarts, S. M., Bertram, J. E. A., Biewener, A. A. 1989. Telemetered in vivo strain analysis of
674 locomotor mechanics of brachiating gibbons. *Nature* 342: 270–272.

675 Thompson, N. E. 2020. The biomechanics of knuckle-walking: 3-D kinematics of the
676 chimpanzee and macaque wrist, hand and fingers. *J. Exp. Biol.* 223: jeb224360.

677 Thorpe, S.K., Crompton, R.H. 2005. Locomotor ecology of wild orangutans (*Pongo*
678 *pygmaeus abelii*) in the Gunung Leuser Ecosystem, Sumatra, Indonesia: A
679 multivariate analysis using log-linear modelling. *Am. J. Phys. Anthropol.* 127: 58–78.

680 Thorpe, S.K., Crompton, R.H. 2006. Orangutan positional behavior and the nature of arboreal
681 locomotion in Hominoidea. *Am. J. Phys. Anthropol.* 131: 384–401.

682 Thorpe, S. K. S., Holder, R., Crompton, R. H. 2009. Orangutans employ unique strategies to
683 control branch flexibility. *Proc. Nat. Acad. Sci. USA* 106: 12646–12651.

684 Tocheri, M. W., Solhan, C. R., Orr, C. M., Femiani, J., Frolich, B., Groves, C. P., Harcourt-
685 Smith, W. E., Richmond, B. G., Shoelson, B., Jungers, W. 2011. Ecological
686 divergence and medial cuneiform morphology in gorillas, *J. Hum. Evol.* 60: 171–184.

687 Tsegai, Z. J., Kivell, T. L., Gross, T., Nguyen, N. H., Pahr, D., Smaers, J., Skinner, M. M.
688 2013. Trabecular bone structure correlates with hand posture and use in Hominoids.
689 *PLoS ONE* 8: e78781.

690 Tsegai, Z. J., Skinner, M. M., Pahr, D. H., Hublin, J.-J., Kivell, T. L. 2018. Systemic patterns
691 of trabecular bone across the human and chimpanzee skeleton. *J. Anat.* 232: 641–656.

692 Tuttle, R.H. 1969. Quantitative and functional studies on the hands of the anthropoidea. I.
693 The Hominoidea. *J. Morphol.* 128: 309–363.

694 Umemura, Y., Sogo, N., Honda, A. 2002. Effects of intervals between jumps or bouts on
695 osteogenic response to loading. *J. Appl. Physiol.* 93: 1345–1348.

696 Wickham, H., François, R., Henry, L., Müller, K. 2018. Dplyr: A grammar of data
697 manipulation. <https://cran.r-project.org/web/packages/dplyr/index.html>

698 Williams, S. A. 2010. Morphological integration and the evolution of knuckle-walking. *J.*
699 *Hum. Evol.* 58: 432–440.

700 Wunderlich, R., Jungers, W. 2009. Manual digital pressures during knuckle-walking in
701 chimpanzees (*Pan troglodytes*). *Am. J. Phys. Anthropol.* 139: 394–403.

702 Youlatos, D. 2008. Locomotion and positional behaviour of spider monkeys. In: Campbell,
703 C. J., editor. *Spider Monkeys: behaviour, ecology and evolution of the genus Ateles*.
704 Cambridge: Cambridge University Press. pp. 185-219.

705 Zihlman, A.L., Mcfarland, R.K., Underwood, C.E. 2011. Functional Anatomy and
706 Adaptation of Male Gorillas (*Gorilla gorilla gorilla*) With Comparison to Male
707 Orangutans (*Pongo pygmaeus*). *Anat. Rec.* 294: 1842–1855.

708 Zylstra, M. 1999. Functional morphology of the hominoid forelimb: implications for
709 knuckle-walking and the origins of hominid bipedalism. Doctoral dissertation,
710 University of Toronto.

711

712 **Figure legends**

713

714 Figure 1. Colour map of differences between taxa in bone volume fraction (BV/TV) and
715 degree of anisotropy (DA) patterns for a representative individual. The original trabecular
716 structure (i.e., a slice from the CT scanned bone) is also presented (Trabeculae).

717

718 Figure 2. Box-and-whisker plots of bone volume fraction (BV/TV) and degree of anisotropy
719 (DA), grouped by genus.

720

721 Figure 3. Bivariate plot of mean values per specimen (at species level) of bone volume
722 fraction (BV/TV) and degree of anisotropy (DA). Convex hulls denote species distribution
723 limits except for those species for which only two specimens are available.

724

725

Table 1. Details of the sample of the study.

Taxon	Common name	N	Side R/L	Sex M/F/Un	Preferred Locomotor Behaviour	Collections/Project and Housing Institution	CT Resolution range in μm
<i>Gorilla gorilla gorilla</i>	Western lowland gorilla	4	2/2	1/3/0	Knuckle-walking	Powell-Cotton Museum (Birchington, UK)	40.7-57.9
<i>Gorilla beringei beringei</i>	Mountain gorilla (Virungas)	3	0/3	1/2/0	Knuckle-walking	Mountain Gorilla Skeletal Project, Dian Fossey Gorilla Fund International's Karisoke Research Centre (Rwanda)	89.8-99.9
<i>Pan troglodytes verus</i>	Common chimpanzee	7	1/6	1/6/0	Knuckle-walking	Tai Forest Collection, Max Planck Institute for Evolutionary Anthropology (Leipzig, Germany)	23.7-30.1
<i>Pongo pygmaeus</i>	Orang-utan	5	2/3	2/3/0	Quadrumanous climbing/clambering	ZMB ¹ , ZMS ²	26.6-28.3
<i>Symphalangus syndactylus</i>	Siamang	3	2/1	0/2/1	Brachiation	ZMB	25.6-27.5
<i>Macaca fascicularis</i>	Long-tailed macaque	3	0/3	0/0/3	Arboreal quadrupedalism	ZMB	23.8-30
<i>Papio hamadryas</i>	Hamadryas baboon	2	1/1	2/0/0	Terrestrial quadrupedalism	ZMB	27.5 (single scan)
<i>Ateles</i> sp.	Spider monkey	4	2/2	1/1/2	Arboreal quadrupedalism	ZMB	24.7-26.5
<i>Alouatta</i> sp.	Howler monkey	2	1/1	1/0/1	Arboreal quadrupedalism	ZMB, ZMS	21.9, 26.5

¹ Museum für Naturkunde – Leibniz Institute for Evolution and Biodiversity Science (Berlin, Germany).

² Zoologische Staatssammlung Munchen (Munich, Germany).

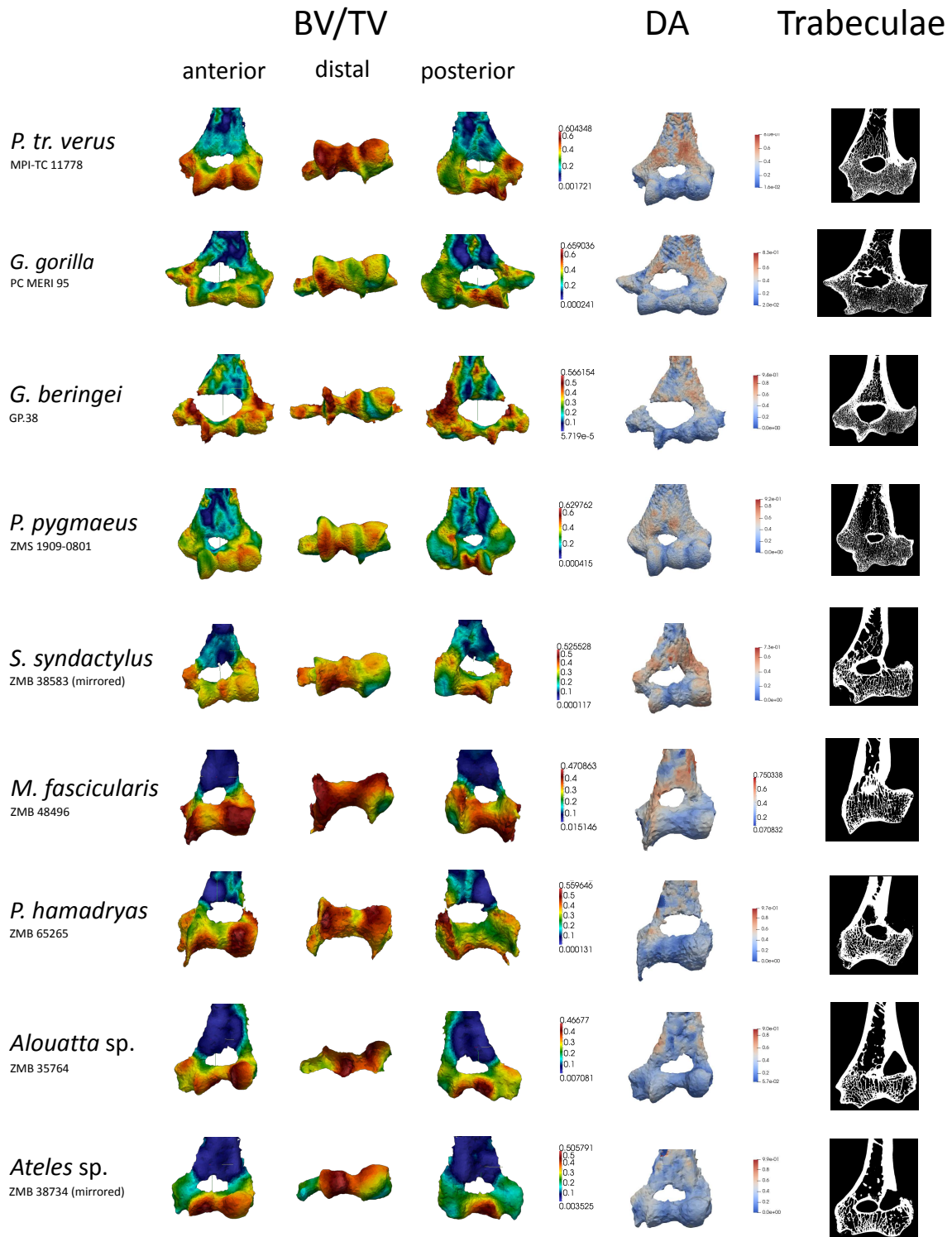


Figure 1.

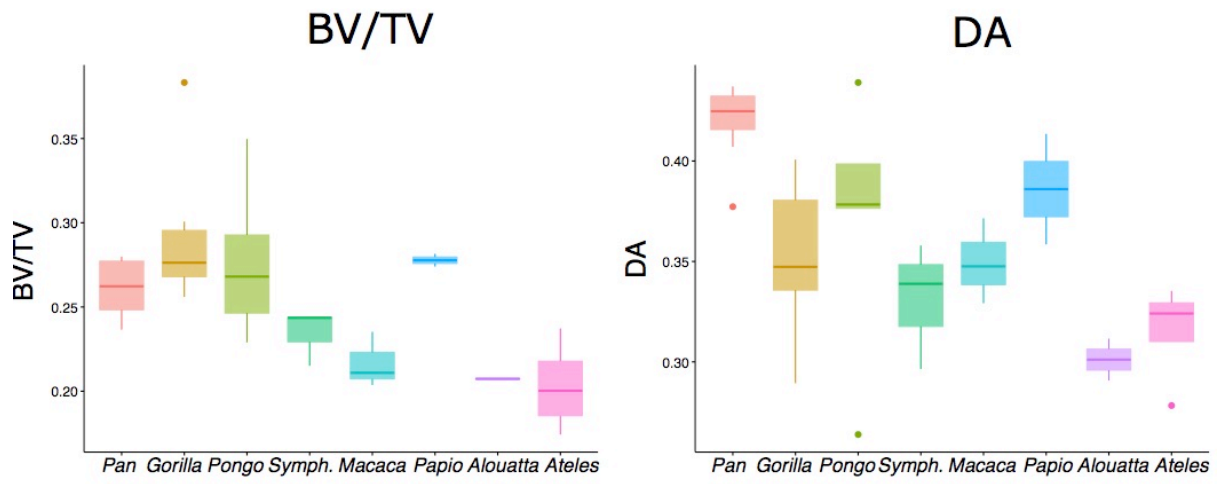


Figure 2.

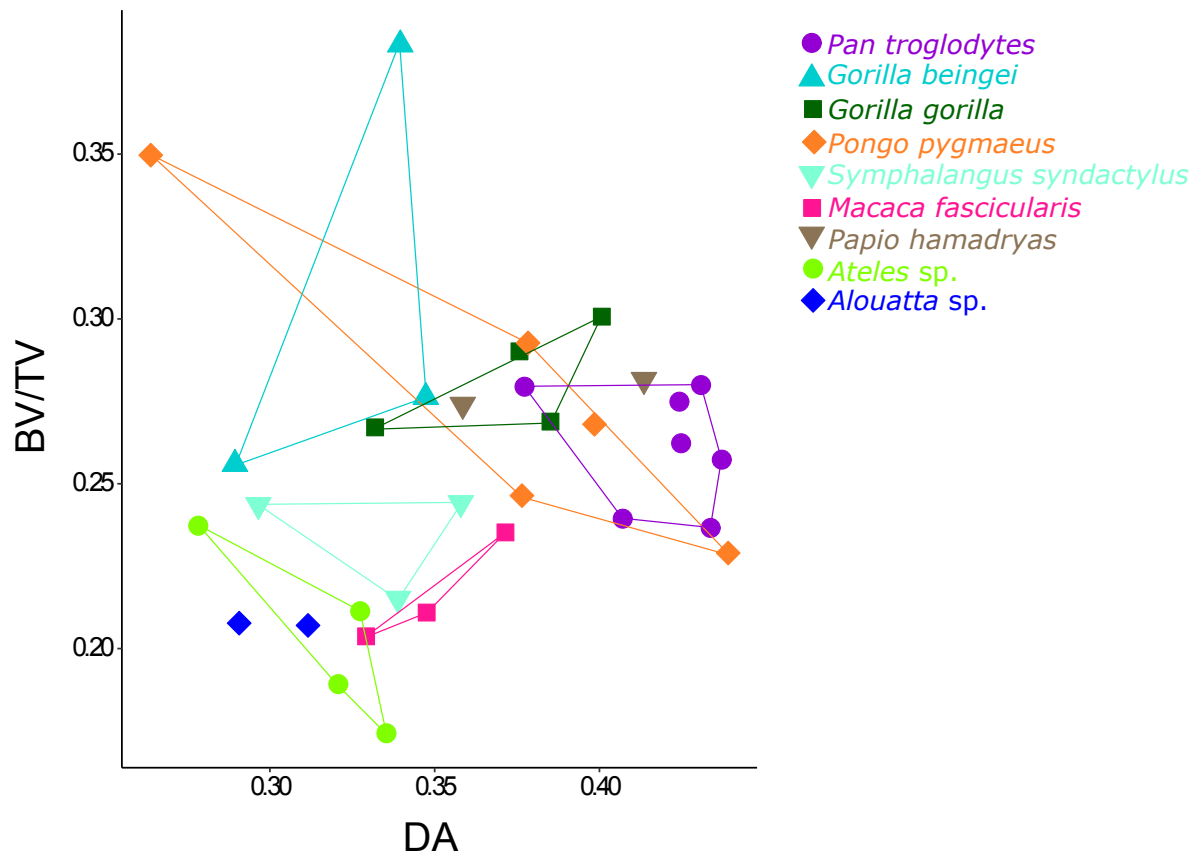


Figure 3.